

# Generalized Receiver with Decision-Feedback Equalizer for Multicode Wideband DS-CDMA

VYACHESLAV TUZLUKOV

Department of Technical Maintenance of Aviation and Radio Electronic Equipment  
Belarusian State Aviation Academy  
77, Uborevicha Str., 220096 Minsk  
BELARUS

*Abstract:* - In the present paper, a chip-level minimum mean-square-error (MMSE) decision-feedback equalizer for the downlink receiver of multicode wideband direct sequence code-division multiple access (DS-CDMA) wireless communication systems over frequency-selective channels is investigated. Firstly, the MMSE per symbol achievable by an optimal decision-feedback equalizer is derived, assuming that all interchip interference (ICI) of the desired user can be eliminated. The MMSE of the decision-feedback equalizer is always less than or at most equal to that of linear equalizers. When all the active codes belong to the desired user, the ideal decision-feedback equalizer is able to eliminate multicode interference and approach the performance of the single-code case at high signal-to-noise ratio (*SNR*) range. Secondly, we apply the hypothesis-feedback equalizer or tentative-chip decision-feedback equalizer in the multicode scenario. The tentative-chip decision-feedback equalizer outperforms the chip-level linear equalizer and the decision-feedback equalizer that only feeds back the symbols already decided. The performance gain increases with *SNR*, but decreases with the number of active codes owned by the other users. When all the active codes are assigned to the desired user, the tentative-chip decision-feedback equalizer eliminates the multicode interference and achieves single-user performance at the high *SNR*, similarly, to the ideal decision-feedback equalizer. The asymptotic performance of the decision-feedback equalizer is confirmed through the bit error rate (*BER*) simulation over various channels.

*Key-Words:* - Generalized receiver, decision-feedback equalizer, frequency-selective fading, intersymbol interference, wideband direct-sequence code-division multiple-access (WDS-CDMA).

Received: July 29, 2021. Revised: July 15, 2022. Accepted: August 21, 2022. Published: September 1, 2022.

## 1 Introduction

Multicode direct-sequence code-division multiple-access (DS-CDMA) technology [1], [2] is the high-speed and multirate wireless communication scheme. Multicode DS-CDMA technology separates the data symbols of a user into several parallel streams and spreads them using different channelization codes. Thus, users with heterogeneous data rates can be supported. Multicode transmission has been incorporated into the five-generation wideband DS-CDMA (WDS-CDMA) physical layer standards [3].

In WDS-CDMA wireless communication systems, the wideband signal incurs significant frequency-selective fading in multipath wireless channels. This frequency-selectivity destroys the orthogonality of the Walsh-Hadamard channelization codes, and causes multiuser access interference and multicode interference as well. In the downlink channel, the multiuser chip signals received by a mobile station are synchronous and suffering the same frequency-selective fading. The channelization codes associated with a given user are known at the receiver. The-

se unique properties may be exploited to obtain detection techniques with the better performance.

It is well-known that the traditional RAKE receiver suffers severely from the multiple access interference and multicode interference. On the other hand, the chip-level downlink linear equalizer demonstrates the better capability in restoring the orthogonality of the channelization codes and suppressing the multiuser access interference. The employment of the linear equalizer in short spreading code systems is discussed in [4] and [5], and in systems with a base station specific long scrambling code is considered in [6]-[8]. Among these papers, [4], [6], and [7] deal with block wise processing, while the rest use an equalizer followed by a code correlator and generate decisions symbol-by-symbol. The advantages of these chip-level linear equalizers include that they only need the knowledge of the desired user's channelization codes, and that their coefficients only need to be computed once if the channel is time-invariant. In [9], a generalized RAKE receiver, which is equivalent to a fractionally-spaced linear equalizer

followed by the code correlator, is proposed to suppress both intersymbol interference and multiuser access interference. Training-based or blind adaptive linear equalizers have appeared in, for instance, [10] and [11].

It has been shown [12], [13] that decision-feedback equalizer can further reduce the effect of the intersymbol interference in the short code case, where the periodic short codes and the physical channel form a combined equivalent channel, and the decision-feedback equalizer can operate on the symbol level. In the downlink of WDS-CDMA wireless communication system, the equivalent symbol-level systems are time-varying because of the aperiodic long scrambling code. As a result, the decision-feedback equalizer has to operate at the chip level. However, feedback chips cannot be reliably determined until the whole symbol has been received. One way to solve this dilemma is to only feedback the chips of the past symbols of the desired user, which we call the past symbol decision-feedback equalizer. The past symbol decision-feedback equalizer cancels the intersymbol interference caused by the already decided symbols, leaving the interchip interference caused by the chips in the current symbol intact. Another decision feedback method is to apply the hypothesis-feedback equalizer [14], which is originally proposed for the single rate short code case and termed the tentative-chip decision-feedback equalizer in this paper. The tentative-chip decision-feedback equalizer feeds back hypothesized chips, rather than actual decisions of multicode symbols of the desired user.

In this paper, we first analyze the symbol-level minimum mean-square-error (MMSE) of an ideal chip-level decision-feedback equalizer assuming that the interchip interference associated with the multicode of the reference user can be completely removed by feeding back all the past chips of the intra user signals. It is found that the ideal decision-feedback equalizer always outperforms the linear equalizer. Furthermore, when the received signal is nothing but the multicode signals of the reference user, the ideal decision-feedback equalizer is able to eliminate the multicode interference and achieves a single-code performance at the sufficiently large signal-to-noise ratio (*SNR*). We then formulate the tentative-chip decision-feedback equalizer in multicode scenario. The simulation of the bit-error rate (*BER*) demonstrates that the tentative-chip decision-feedback equalizer does achieve the single-code performance at the high *SNR* range when all the active codes are assigned to the reference user.

The rest of this paper is organized as follows. The system model is described in Section 2. The genera-

lized receiver and its main functioning principles are presented in Section 3. The MMSE of the ideal decision-feedback equalizer is analysed in Section 4. The tentative-chip decision-feedback equalizer in multicode case is formulated in Section 5, together with a brief revisit of past symbol decision-feedback equalizer. Numerical comparisons of the performance of different equalizers are contained in Sections 4 and 5. Conclusions are given in Section 6.

## 2 System Model

Consider the downlink of a single-cell multicode DS-CDMA wireless communication system presented in Fig. 1. Data sequences are spread by orthogonal channelization codes and then scrambled by a scrambling code. Orthogonal variable spreading factor [15] codes can adjust spreading factors according to users' data rates. Sometimes multiple channelization codes can be assigned to the same user to further increase the data rate. Without loss of generality, we assume that all users have the same spreading factor  $N_c$  and some users may be assigned multiple codes. Denote active channelization codes as  $c_n^{(j)}$ , for  $n = 0, 1, \dots, N_c - 1$  and  $j = 0, 1, \dots, N_u - 1$ , where  $N_u$  is the number of active channelization codes. Throughout this paper, it is assumed that the desired user is assigned the first  $N_d$  codes  $c_n^{(j)}$ ,  $j = 0, 1, \dots, N_d - 1$ .

The chip sequence spread by the  $j$ -th code is given by

$$x_n^{(j)} = s_n \sum_{m=0}^{N_s-1} b_m^{(j)} c_{n-N_c m}^{(j)}, \quad n = 0, 1, 2, \dots \quad (1)$$

where  $s_n$  is the base station specific scrambling long code,  $b_m^{(j)}$  is the  $m$ -th symbol associated with the  $j$ -th channelization code, assumed to be binary ( $\pm 1$ ) in this paper, and  $N_s$  is the number of symbols transmitted during a given time window. The data symbols of the desired user are serial-to-parallel converted, spread by the assigned set of codes, added with chip sequences of other users, and scrambled by the long code to form the composite multiuser chip signal

$$x_n = \sum_{j=0}^{N_u-1} x_n^{(j)}. \quad (2)$$

Assume that there is no power control at the base station; therefore, the chip signals of all active codes have the same energy.

Furthermore, three assumptions of the codes and symbols are made:

- the long scrambling code is assumed to be an independent identically distributed (i.i.d.) sequence with unit variance:  $E[s_n s_m^*] = \delta_{m-n}$  for the convenience of analysis;
- different channelization codes are orthogonal, i.e.

$$\sum_{n=0}^{N_c-1} c_n^{(j)} c_n^{(k)} = N_c \delta_{j-k} ; \quad (3)$$

- the data symbol associated with the  $j$ -th channelization code  $\{b_m^{(j)}\}$  is a zero-mean unit-variance i.i.d. sequence, and independent from data symbols associated with other channelization codes:

$$E[b_m^{(j)} b_n^{(k)*}] = \delta_{m-n} \delta_{j-k} . \quad (4)$$

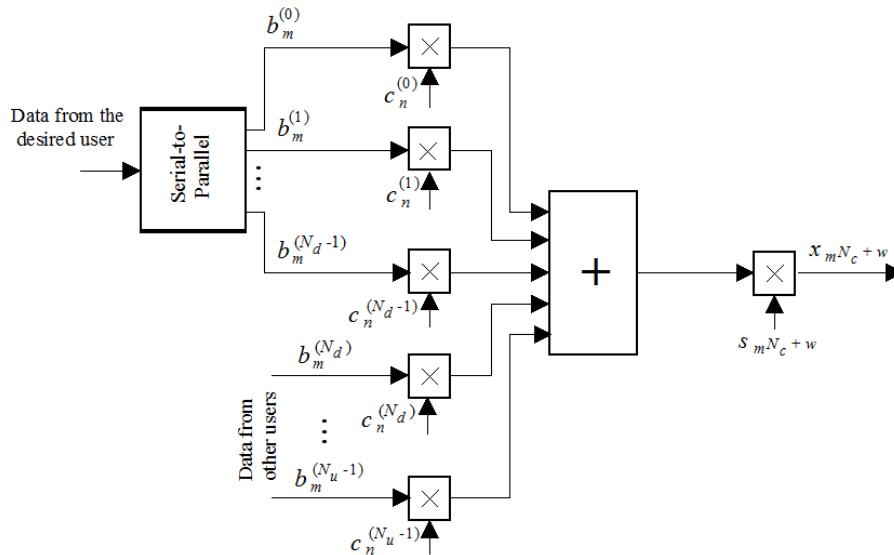


Fig.1. Base station transmitter block diagram of the multicode DS-CDMA wireless communication system.

The impulse response of the channel between the base station transmitter and the mobile station receiver takes the form:

$$h(t) = \sum_{k=0}^{N_a-1} h_k p(t - \tau_k) , \quad (5)$$

where  $N_a$  is the total number of multipaths;  $h_k$  and  $\tau_k$  are the complex fading factor and propagation delay of the  $k$ -th path, respectively;  $p(t)$  is the transmitter pulse shaping waveform, having a square-root raised-cosine spectrum. Note that the chip energy per active code in (1) is normalized to the unit; the actual chip energy is absorbed into channel impulse response in (5). A quasistatic channel model is used in this paper, i.e.,  $h_k$ 's are the constant within a time slot and Rayleigh fading independently from frame to frame.

The signal received by the mobile station takes the form

$$y(t) = \sum_n x_n h(t - nT_c) + w(t) , \quad (6)$$

where  $T_c$  is the chip period and  $w(t)$  is the additive white Gaussian noise (AWGN) with zero-mean and variance  $\sigma_w^2$ . In this paper, the channel state information, the noise power, and the number of active codes are assumed known at the receiver.

### 3 Generalized Receiver: Main Functioning Principles

The generalized receiver is constructed in accordance with the generalized approach to signal processing in noise [16]-[18]. The generalized approach to signal processing in noise introduces an additional noise source that does not carry any information about the parameters of desired transmitted signal with the purpose to improve the signal processing system performance. This additional noise can be considered as the reference noise without any information about the parameters of the signal to be detected.

The jointly sufficient statistics of the mean and variance of the likelihood function is obtained under the generalized approach to signal processing in noise employment, while the classical and modern sig-



AF bandwidth and central frequency can be assigned, too (this bandwidth can-not be used by the transmitted signal because it is out of its spectrum). The case when there are interfering signals within the GR AF bandwidth, the action of this interference on the GR detection performance, and the case of no ideal condition when the noise at the GR PF and GR AF outputs is not the same by statistical parameters are discussed in [21] and [22].

Under the hypothesis  $\mathcal{H}_1$  (“a yes” transmitted signal), the GR CD generates the signal component  $s_i^m[k]s_i[k]$  caused by interaction between the model signal  $s_i^m[k]$ , forming at the MSG output, and the incoming signal  $s_i[k]$ , and the noise component  $s_i^m[k] \times \zeta_i[k]$  caused by interaction between the model signal  $s_i^m[k]$  and the noise  $\zeta_i[k]$  at the PF output. GR ED generates the transmitted signal energy  $s_i^2[k]$  and the random component  $s_i[k]\zeta_i[k]$  caused by interaction between the transmitted signal  $s_i[k]$  and the noise  $\zeta_i[k]$  at the PF output. The main purpose of the GR CC is to cancel completely in the statistical sense the GR CD noise component  $s_i^m[k]\zeta_i[k]$  and the GR ED random component  $s_i[k]\zeta_i[k]$  based on the same nature of the noise  $\zeta_i[k]$ . The relation between the transmitted signal to be detected  $s_i[k]$  and the model signal  $s_i^m[k]$  is defined as:

$$s_i^m[k] = \mu s_i[k], \quad (8)$$

where  $\mu$  is the coefficient of proportionality.

The main functioning condition under the GR employment in any signal processing system including the communication one with radar sensors is the equality between the parameters of the model signal  $s_i^m[k]$  and the incoming signal  $s_i[k]$ , for example, by amplitude. Under this condition it is possible to cancel completely in the statistical sense the noise component  $s_i^m[k]\zeta_i[k]$  of the GR CD and the random component  $s_i[k]\zeta_i[k]$  of the GR ED. Satisfying the GR main functioning condition given by (8),  $s_i^m[k] = s_i[k]$ ,  $\mu = 1$ , we are able to detect the transmitted signal with the high probability of detection at the low SNR and define the transmitted signal parameters with the required high accuracy.

Practical realization of the condition (8) at  $\mu \rightarrow 1$  requires increasing in the complexity of GR structure and, consequently, leads us to increasing in computation cost. For example, there is a need to employ the amplitude tracking system or to use the off-

line data samples processing. Under the hypothesis  $\mathcal{H}_0$  (“a no” transmitted signal), satisfying the main GR functioning condition (8) at  $\mu \rightarrow 1$  we obtain only the background noise  $\eta_i^2[k] - \zeta_i^2[k]$  at the GR output.

Under practical implementation, the real structure of GR depends on specificity of signal processing systems and their applications, for example, the radar sensor systems, adaptive wireless communication systems, cognitive radio systems, satellite communication systems, mobile communication systems and so on. In the present paper, the GR circuitry (Fig.2) is demonstrated with the purpose to explain the main functioning principles. Because of this, the GR flowchart presented in the paper should be considered under this viewpoint. Satisfying the GR main functioning condition (8) at  $\mu \rightarrow 1$ , the ideal case, for the wireless communication systems with radar sensor applications we are able to detect the transmitted signal with very high probability of detection and define accurately its parameters.

In the present paper, we discuss the GR implementation in the broadband space-time spreading MC DS-CDMA wireless communication system. Since the presented GR test statistics is defined by the signal energy and noise power, the equality between the parameters of the model signal  $s_i^m[k]$  and transmitted signal to be detected  $s_i[k]$ , in particular by amplitude, is required that leads us to high circuitry complexity in practice.

For example, there is a need to employ the amplitude tracking system or off-line data sample processing. Detailed discussion about the main GR functioning principles if there is no a priori information and there is an uncertainty about the parameters of transmitted signal, i.e., the transmitted signal parameters are random, can be found in [16], [17, Chapter 6, pp.611–621 and Chapter 7, pp. 631–695].

The complete matching between the model signal  $s_i^m[k]$  and the incoming signal  $s_i[k]$ , for example by amplitude, is a very hard problem in practice because the incoming signal  $s_i[k]$  depends on both the fading and the transmitted signal parameters and it is impractical to estimate the fading gain at the low SNR. This matching is possible in the ideal case only. The GD detection performance will be deteriorated under mismatching in parameters between the model signal  $s_i^m[k]$  and the transmitted signal  $s_i[k]$  and the impact of this problem is discussed in [23]-[26], where a complete analysis about the violation of the main GR functioning requirements is presented. The GR decision statistics requires an estimati-

on of the noise variance  $\sigma_\eta^2$  using the reference noise  $\eta_i[k]$  at the AF output.

Under the hypothesis  $\mathcal{H}_1$ , the signal at the GR PF output, see Fig. 2, can be defined as

$$x_i[k] = s_i[k] + \zeta_i[k] , \quad (9)$$

where  $\zeta_i[k]$  is the noise at the PF output and

$$s_i[k] = h_i[k]s[k] , \quad (10)$$

where  $h_i[k]$  are the channel coefficients. Under the hypothesis  $\mathcal{H}_0$  and for all  $i$  and  $k$ , the process  $x_i[k] = \zeta_i[k]$  at the PF output is subjected to the complex Gaussian distribution law and can be considered as the i.i.d. process.

In the ideal case, we can think that the signal at the GR AF output is the reference noise  $\eta_i[k]$  with the same statistical parameters as the noise  $\zeta_i[k]$ . In practice, there is a difference between the statistical parameters of the noise  $\eta_i[k]$  and  $\zeta_i[k]$ . How this difference impacts on the GR detection performance is discussed in detail in [17, Chapter 7, pp. 631-695] and in [23]-[29].

The decision statistics at the GR output presented in [19] and [20, Chapter 3] is extended for the case of antenna array when an adoption of multiple antennas and antenna arrays is effective to mitigate the negative attenuation and fading effects. The GR decision statistics can be presented in the following form:

$$T_{GR}(\mathbf{X}) = \sum_{k=0}^{N-1} \sum_{i=1}^M 2x_i[k]s_i^m[k] - \sum_{k=0}^{N-1} \sum_{i=1}^M x_i^2[k] + \sum_{k=0}^{N-1} \sum_{i=1}^M \eta_i^2[k] \underset{\mathcal{H}_0}{\overset{\mathcal{H}_1}{>}} \underset{\mathcal{H}_0}{<} THR_{GR} , \quad (11)$$

where

$$\mathbf{X} = [\mathbf{x}(0), \dots, \mathbf{x}(N-1)] \quad (12)$$

is the vector of the random process at the GR PF output and  $THR_{GR}$  is the GR detection threshold.

Under the hypotheses  $\mathcal{H}_1$  and  $\mathcal{H}_0$  when the amplitude of the transmitted signal is equal to the amplitude of the model signal,  $s_i^m[k] = s_i[k]$ ,  $\mu = 1$ , the GR decision statistics  $T_{GD}(\mathbf{X})$  takes the following form in the statistical sense, respectively:

$$\begin{cases} \mathcal{H}_1 : T_{GD}(\mathbf{X}) = \sum_{k=0}^{N-1} \sum_{i=1}^M \{s_i^2[k] + \eta_i^2[k] - \zeta_i^2[k]\} \\ \mathcal{H}_0 : T_{GD}(\mathbf{X}) = \sum_{k=0}^{N-1} \sum_{i=1}^M \{\eta_i^2[k] - \zeta_i^2[k]\} \end{cases} . \quad (13)$$

In (13) the term  $\sum_{k=0}^{N-1} \sum_{i=1}^M s_i^2[k] = E_s$  corresponds to the average transmitted signal energy, and the term  $\sum_{k=0}^{N-1} \sum_{i=1}^M \eta_i^2[k] - \sum_{k=0}^{N-1} \sum_{i=1}^M \zeta_i^2[k]$  is the background noise at the GR output. The GR output background noise is the difference between the noise power at the GR PF and GR AF outputs. Practical implementation of the GR decision statistics requires an estimation of the noise variance  $\sigma_\eta^2$  using the reference noise  $\eta_i[k]$  at the AF output.

## 4 Ideal Decision-Feedback Equalizer

In this section, we evaluate the symbol-level MMSE of an ideal chip-level decision-feedback equalizer, and compare it with the MMSE of ideal linear equalizer. By ideal, we mean that the receive filters can be of infinite length and noncausal.

### 4.1 Solution of Ideal Decision-Feedback Equalizer

To derive the MMSE of decision-feedback equalizer with the ideal receive filters, we assume that the decision-feedback equalizer can always make correct decisions on the chips corresponding to the desired codes and feed them back. Hence, the post cursor interchip interference caused by the desired codes can be eliminated.

The receiver structure of the desired user is presented in Fig. 3. The received signal is first filtered by  $g(t)$  and then sampled at chip rate. The previously decided chips are filtered by a discrete-time filter  $f_n$  and subtracted from the received samples. The resultant chip samples are then despread and descrambled to give the symbol estimates  $\hat{b}_m^{(j)}$ ,  $j = 0, 1, \dots, N_d - 1$ , where the notation  $(\cdot)$  stands for an estimate of the quantity in parentheses.

The MMSE decision-feedback equalizer is designed to minimize the following mean-square-error

$$E | \hat{b}_k^{(j)} - b_k^{(j)} |^2 , \quad j \in \{0, 1, \dots, N_d - 1\} . \quad (14)$$

Since the mean-square-error is independent of the channelization code index  $j$ , we will focus on the mean-square-error associated with the zero-th code.

Let

$$\begin{cases} d(t) = h(t) * g(t), \\ \rho(t) = w(t) * g(t), \end{cases} \quad (15)$$

where the operator  $*$  denotes a convolution. Their chip rate samples are defined as

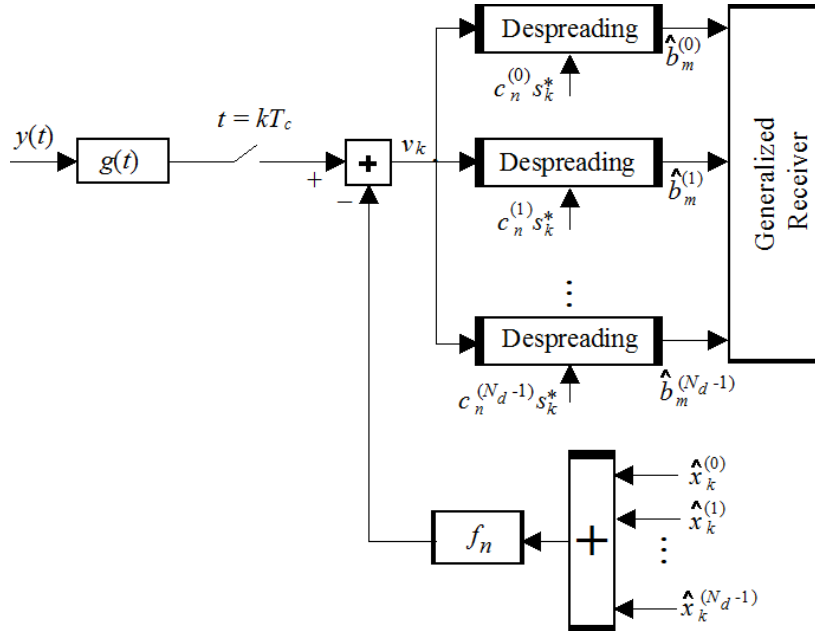


Fig. 3. Block diagram of the receiver

$$d_n = d(nT_c) = \int_{-\infty}^{\infty} g(\tau)h(nT_c - \tau)d\tau \quad (16)$$

and  $\rho_n = \rho(nT_c)$ . At this point, we make an assumption that the decisions on past chips of the desired user are all correct, whose legitimacy will be clear in Section 5.2. With this assumption, the received sample at the time

$$t = (qN_c + k)T_c \quad (17)$$

takes the form

$$v_{qN_c+k} = \sum_n d_n x_{qN_c+k-n} - \sum_{n=1}^{\infty} f_n \sum_{p=0}^{N_d-1} x_{qN_c+k-n}^{(p)}. \quad (18)$$

The symbol estimate after despreading is

$$\hat{b}_q^{(0)} = \frac{1}{N_c} \sum v_{qN_c+k} c_k^{(0)} s_{qN_c+k}^*, \quad (19)$$

where the symbol  $(\cdot)^*$  denotes the complex conjugation. The mean-square-error of decision-feedback equalizer is then by definition

$$MSE_{DFE} = E \left| (d_0 - 1) \hat{b}_q^{(0)} + 1/N_c \right|^2$$

$$\begin{aligned} & \times \left\{ \sum_{k=0}^{N_c-1} \sum_{p=0}^{N_d-1} \sum_{n=1}^{\infty} (d_n - f_n) x_{qN_c+k-n}^{(p)} c_k^{(0)} s_{qN_c+k}^* \right. \\ & \quad \left. + \sum_{k=0}^{N_c-1} \sum_{p=0}^{N_d-1} \sum_{n=1}^{\infty} d_n x_{qN_c+k-n}^{(p)} c_k^{(0)} s_{qN_c+k}^* \right. \\ & \quad \left. + \sum_{k=0}^{N_c-1} \sum_{n=-\infty}^{-1} d_n x_{qN_c+k-n}^{(p)} c_k^{(0)} s_{qN_c+k}^* + \sum_{k=0}^{N_c-1} \rho_{qN_c+k} c_k^{(0)} s_{qN_c+k}^* \right\}^2 \quad (20) \end{aligned}$$

A straightforward calculation yields

$$\begin{aligned} MSE_{DFE} &= |d_0 - 1|^2 + \frac{\mathcal{N}_0}{N_c} \int_{-\infty}^{\infty} |g(\tau)|^2 d\tau \\ & \quad + \frac{N_u - N_d}{N_c} \sum_{n=1}^{\infty} |d_n|^2 + \frac{N_u}{N_c} \sum_{n=-\infty}^{-1} |d_n|^2 \\ & \quad + \frac{N_d}{N_c} \sum_{n=1}^{\infty} |d_n - f_n|^2. \quad (21) \end{aligned}$$

It can be immediately concluded from the last term in the above equation that the mean-square-error is minimized by setting  $f_n = d_n, n=1,2,\dots$

The problem now becomes to find  $g(t)$  that minimizes

$$MSE_{DFE} = |d_0 - 1|^2 + \frac{1}{N_c} \left[ \mathcal{N}_0 \int_{-\infty}^{\infty} |g(\tau)|^2 d\tau + (N_u - N_d) \sum_{n=1}^{\infty} |d_n|^2 + N_u \sum_{n=-\infty}^{-1} |d_n|^2 \right]. \quad (22)$$

The above expression indicates that in the general case, under the assumption of perfect past decisions, the mean-square error is contributed by both precursors and post cursors in the overall impulse response  $d(t)$ . The receiver of the desired user only feeds back the chip signals of  $N_d$  codes among all  $N_u$  active codes. This is different from the single-user decision-feedback equalizer case, where the mean-square-error only consists of precursors in  $d(t)$ .

We now find a precise solution to the problem in (22). As shown in Appendix I, using a calculus-of-variation, we can obtain an integral equation for  $g(t)$

$$N_c h(-t) = N_c h(-t) \int_{-\infty}^{\infty} g^*(\tau) h^*(-\tau) d\tau + N_u \sum_{n=-\infty}^{-1} h(nT_c - t) \times \int_{-\infty}^{\infty} g^*(\tau) h^*(nT_c - \tau) d\tau + \mathcal{N}_0 g^*(t) + (N_u - N_d) \times \sum_{n=1}^{\infty} h(nT_c - t) \int_{-\infty}^{\infty} g^*(\tau) h^*(nT_c - \tau) d\tau. \quad (23)$$

Taking complex conjugation of both sides of (23), followed by multiplying both sides by  $h(kT_c - t)$ , then integrating from minus to plus infinity over variable  $t$ , we can obtain a set of linear equations involving  $\{d_n\}$

$$N_c r_k = N_c r_k d_0 + \mathcal{N}_0 d_k + N_u \sum_{n=-\infty}^{-1} r_{k-n} d_n + (N_u - N_d) \sum_{n=1}^{\infty} r_{k-n} d_n \quad (24)$$

for  $k = 0, \pm 1, \pm 2, \dots$ , where

$$r_k = \int_{-\infty}^{\infty} h(kT_c - \tau) h^*(-\tau) d\tau. \quad (25)$$

Let us define the  $z$ -transforms of the sequences  $\{d_n\}_{-\infty}^{\infty}$  and  $\{r_n\}_{-\infty}^{\infty}$ , respectively, as

$$D(z) = \sum_{n=-\infty}^{\infty} d_n z^{-n}, \quad (26)$$

$$R(z) = \sum_{n=-\infty}^{\infty} r_n z^{-n}. \quad (27)$$

Define

$$\Gamma(z) = \frac{N_u R(z) + \mathcal{N}_0}{(N_u - N_d) R(z) + \mathcal{N}_0}. \quad (28)$$

Since  $\Gamma(z)$  is a rational valid power spectrum density, it has a monic minimum-phase spectral factorization [30], written as

$$\Gamma(z) = \gamma^2 \mathcal{M}(z) \mathcal{M}^*(z^{-1}). \quad (29)$$

where  $\gamma^2$  is the geometric average [30] of  $\Gamma(z)$ , that is

$$\gamma^2 = \langle \Gamma(z) \rangle_{\mathcal{G}} = \exp \left\{ \frac{1}{2\pi} \int_{-\pi}^{\pi} \log \Gamma[\exp(j\omega)] d\omega \right\} \quad (30)$$

and  $\mathcal{M}(z)$  is a monic, causal, and minimum-phase sequence. It is derived in Appendix II that the solution of (24) in terms of the  $z$ -transform of the sequence  $\{d_n\}_{-\infty}^{\infty}$  is

$$D(z) = \frac{N_c N_d R(z)}{N_d + (N_c - N_u)(1 - \gamma^{-2}) \gamma^2 \mathcal{M}^*(z^{-1})} \times \frac{1}{(N_u - N_d) R(z) + \mathcal{N}_0}. \quad (31)$$

Conjugating both sides of (23), collecting terms, and using the definition of  $\{d_n\}$  in (16), we can obtain the forward filter of minimum mean-square-error chip-level decision-feedback equalizer

$$g(t) = \frac{N_c}{\mathcal{N}_0} (1 - d_0) h^*(-t) - \frac{N_u}{\mathcal{N}_0} \sum_{n=-\infty}^{-1} d_n h^*(nT_c - t) - \frac{N_u - N_d}{\mathcal{N}_0} \sum_{n=1}^{\infty} d_n h^*(nT_c - t) = \left[ \frac{N_c (1 - d_0) \delta(t)}{\mathcal{N}_0} - \frac{N_u}{\mathcal{N}_0} \sum_{n=-\infty}^{-1} d_n \delta(t - nT_c) - \frac{N_u - N_d}{\mathcal{N}_0} \sum_{n=1}^{\infty} d_n \delta(t - nT_c) \right] * h^*(-t), \quad (32)$$

where  $\delta(t)$  is the Dirac delta-function. From (32), the forward filter of the receiver consists of a matched filter and a non-causal chip rate tapped-delay line filter.

From the optimum receiving filter, we now obtain the minimum mean-square-error. Multiplying

both sides of (32) by  $g^*(t)$  and integrating from  $-\infty$  to  $\infty$ , we have

$$N_c(d_0 - |d_0|^2) = \mathcal{N}_0 \int_{-\infty}^{\infty} |g_0(\tau)|^2 d\tau + N_u \sum_{n=-\infty}^{-1} |d_n|^2 + (N_u - N_d) \sum_{n=1}^{\infty} |d_n|^2. \quad (33)$$

Substituting (33) into (22), we get a formula for the minimum mean-square-error

$$MMSE_{DFE}(N_d) = 1 - d_0^* = 1 - \frac{N_c}{N_d \gamma^2 (\gamma^2 - 1)^{-1} + N_c - N_u}, \quad (34)$$

where we have used the notation  $MMSE_{DFE}(N_d)$  to emphasize the dependence of  $MMSE$  on  $N_d$ . It is proved in Appendix III that  $MMSE_{DFE}(N_d)$  is a non-increasing function of  $N_d$ . This is because with more active codes belonging to the desired user, the receiver can cancel more interchip interference and get a smaller minimum mean-square-error.

It can be shown that  $MMSE_{DFE}(N_d)$  increases with the number of active codes  $N_u$ . However,  $MMSE_{DFE}(N_u)$  approaches  $MMSE_{DFE}(1)$  as the  $SNR$  increases. To see this, evaluating (23) with  $N_u = N_d$ , where  $1 \leq N_u \leq N_c$  and  $N_u = N_d = 1$ , respectively, we have

$$MMSE_{DFE}(N_u) = \frac{N_u}{N_c \langle N_u \mathcal{N}_0^{-1} R(z) + 1 \rangle_{\mathcal{G}} - (N_c - N_u)} \quad (35)$$

and

$$MMSE_{DFE}(1) = \frac{1}{\langle N_c \mathcal{N}_0^{-1} R(z) + N_c \rangle_{\mathcal{G}} - N_c + 1}. \quad (36)$$

From (35) and (36)

$$\lim_{\mathcal{N}_0 \rightarrow 0} \frac{MMSE_{DFE}(N_u)}{MMSE_{DFE}(1)} = 1. \quad (37)$$

In other words, when all the active channelization codes belong to the reference user, the ideal decision-feedback equalizer approaches single-code performance in high  $SNR$  range. That means the ideal decision-feedback equalizer can asymptotically eliminate multicode interference. Meanwhile, it is noticeable that some interchip interference still exists at the output of the ideal decision-feedback equalizer, even in the single-code case. This is because the

feedback filter only cancels the post cursors intersymbol interference or interchip interference, and the forward filter seeks a trade off between precursor suppression and noise amplification. Therefore, the precursor is not eliminated, but largely suppressed.

## 4.2 Comparison with Ideal Linear Equalizer

To compare the chip-level decision feedback equalizer and linear equalizer we define

$$\Theta(z) = \frac{(N_u - 1)R(z) + \mathcal{N}_0}{N_u R(z) + \mathcal{N}_0} \quad (38)$$

and its arithmetic average [30]

$$\theta^2 = \langle \Theta(z) \rangle_{\mathcal{A}} = \frac{1}{2\pi} \int_{-\pi}^{\pi} \Theta[\exp(j\omega)] d\omega. \quad (39)$$

Similarly, to the derivation of the decision feedback equalizer, the symbol-level minimum mean-square error of the chip-level linear equalizer can be presented in the following form

$$MMSE_{LE} = 1 - \frac{N_c}{1/(1 - \theta^2) + N_c - N_u}. \quad (40)$$

We next show that the following relationship always holds:

$$MMSE_{LE} \geq MMSE_{DFE}(1), \quad (41)$$

i.e., even if only one active code is associated with the desired user, the decision feedback equalizer is still better than the linear equalizer. At  $N_d = 1$ ,  $\Gamma(z)$  in (28), and  $\Theta(z)$  in (38) are related by  $\Theta(z) = 1/\Gamma(z)$ . Therefore,

$$MMSE_{DFE}(1) = \frac{N_c}{1/(1 - \langle \Theta(z) \rangle_{\mathcal{G}}) + N_c - N_u}. \quad (42)$$

For any valid power spectrum density function  $\Theta(z)$ , we have [30]

$$\langle \Theta(z) \rangle_{\mathcal{G}} \leq \langle \Theta(z) \rangle_{\mathcal{A}}. \quad (43)$$

Now, comparing (40) and (42), it is easy to show that (41) holds.

## 4.3 Numerical Results

In this section, we compare the minimum mean-square error of the ideal decision feedback equalizer with that of the linear equalizer and RAKE receiver through numerical results. For fairness, the RAKE receiver is scaled by a scalar that is chosen to minimize the symbol-level mean-squared error. We first consider a fixed channel [31]. In the notation defi-

ned in (5), the channel has  $N_a = 5$  multipaths, with the propagation delay  $\tau_k = kT_c, k = 0, 1, \dots, 4$  and  $h_k, k = 0, 1, \dots, 4$ , as shown in Fig. 4. The chip period is  $T_c = 0.26 \mu s$  [3], and the roll-off factor of the square-root raised-cosine waveform  $p(t)$  is 0.22 [18]. Throughout the numerical example in this paper, the spreading factor is  $N_c = 4$ . Two cases of active code number are shown in Fig. 5: at  $N_u = 4$  we compare  $MMSE_{LE}, MMSE_{DFE}(1)$ , and  $MMSE_{DFE}(4)$ ; at  $N_u = 1$ , we show  $MMSE_{DFE}(1)$ . Here, SNR per symbol is defined as

$$SNR = \frac{N_c E |b_m^{(0)} s_n c_{n-N_c m}^{(0)}|^2 \sum_k E |h(kT_c)|^2}{\mathcal{N}_0} \quad (44)$$

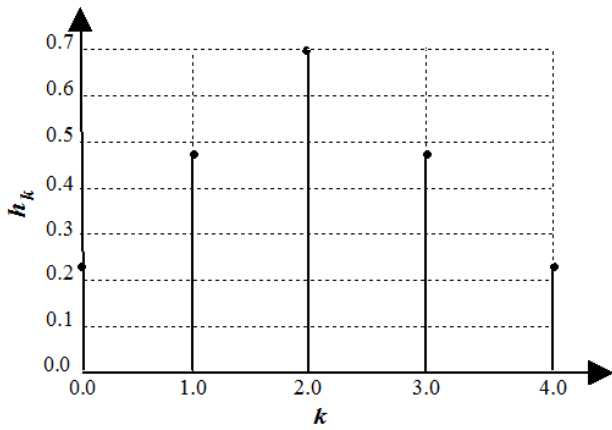


Fig. 4. Fixed channel.

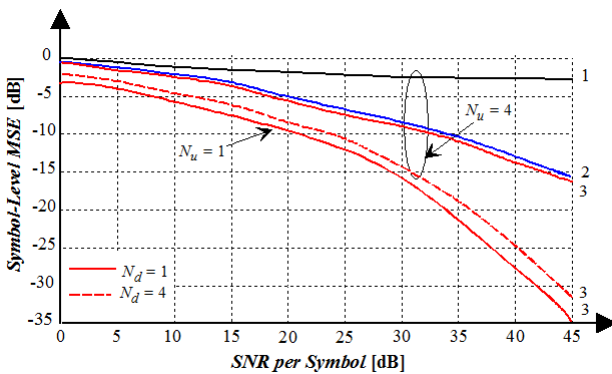


Fig. 5. Comparison of the minimum mean square error for: 1- RAKE receiver; 2- linear equalizer; 3- decision feedback equalizer:  $N_d = 1, 4$ .

The large gap between  $MMSE_{DFE}(4)$  and  $MMSE_{DFE}(1)$ , or  $MMSE_{LE}$  reveals the decision feedback equalizer's ability to suppress the multicode interference when the desired user has multiple active codes. As SNR increases, the curve for  $MMSE_{DFE}(4)$

when  $N_u = 4$  approaches the curve for  $MMSE_{DFE}(1)$  at  $N_u = 1$ , which confirms our asymptotic analysis. Meanwhile, the RAKE receiver shows a high error floor compared with all equalizers.

Figure 6 demonstrates the impact of  $N_u$  on the minimum mean-squared error. In the case of the decision feedback equalizer,  $N_d$  is fixed to be one. From Fig. 6, when the desired user has only one active code, the performance advantage of the decision feedback equalizer over the linear equalizer decreases as the number of active codes (users) increases. This is because the decision feedback equalizer leaves the interchip interference of the other users' chip signal intact and the multiple access interference become dominant interference source. The RAKE receiver has an error floor even when  $N_u = 1$ , showing that the RAKE is sensitive to intersymbol interference or interchip interference.

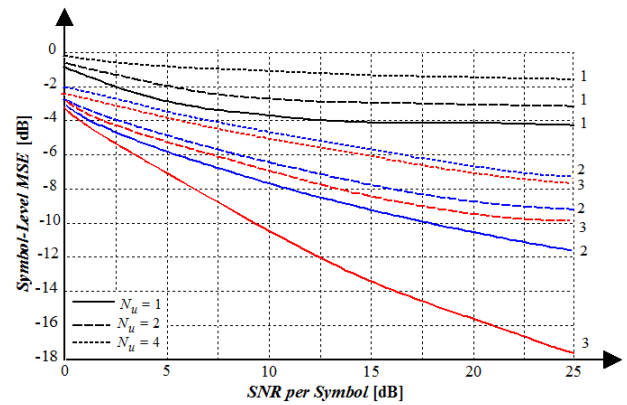


Fig. 6. Comparison of the minimum mean squared error for  $N_u = 1, 2$  and  $4, N_d = 1$ ; 1 - RAKE receiver; 2 - linear equalizer; 3- decision feedback equalizer.

Table I. Universal mobile telecommunication system indoor office channel B tapped-delay-line parameters

Relative Delay (ns)	0	100	200	300	500	700
Average Power (dB)	0	-3.6	-7.2	-10.8	-18.0	-25.2

Figure 7 demonstrates the performance of the decision feedback equalizer averaged over 1000 random realizations of universal mobile telecommunication system indoor office type B channels [19], whose tapped-delay-line parameters are tabulated in Table I. Here, the number of multipaths  $N_a$  and path delays  $\tau_k, k = 0, 1, \dots, N_a - 1$  are the set according to [19], while the fading factors  $h_k, k = 0, 1, \dots, N_a - 1$  are the Gaussian random variables with the zero mean

and variance equal to the average power of each tap as specified in [19]. The number of active codes is  $N_u = 4$ . From Fig. 7 we see that when the SNR is 20 dB,  $MMSE_{DFE}$  (4) is 1.9 dB smaller than  $MMSE_{LE}$ .

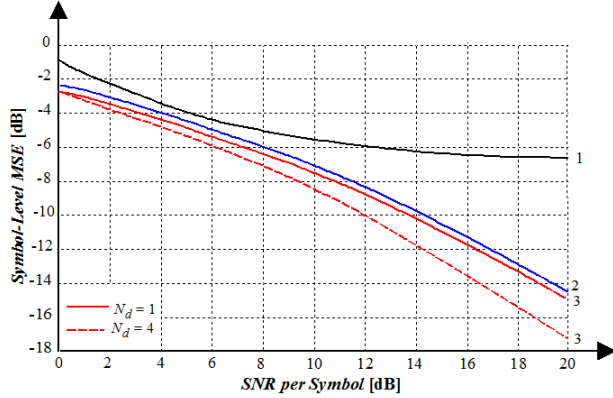


Fig.7 . Comparison of the minimum mean squared error for: 1 - RAKE; 2 - linear equalizer; 3 - decision feedback equalizer  $N_d = 1,4$  over the universal mobile telecommunication system indoor office type B channels.

## 5 Tentative Chip Decision Feedback Equalizer

### 5.1 Receive Generalized Receiver Output

The received signal passes through the generalized receiver, in which the GR PF is matched with  $p(t)$ . The output of the generalized receiver takes the following form

$$\bar{y}(t) = \sum_n [2x_n(t)\hat{s}^m(t - nT_c) - x_n(t)x^*(t - nT_c) + \hat{\zeta}_n(t)] , \quad (45)$$

where

$$\varsigma_n(t) = \eta(t)\eta^*(t - nT_c) - \zeta(t)\zeta^*(t - nT_c); \quad (46)$$

$$\hat{s}^m(t - nT_c) = s^m(t) * p^*(-t); \quad (47)$$

$$\hat{\zeta}_n(t) = \varsigma_n(t) * p^*(-t) . \quad (48)$$

A discrete-time channel model can be obtained by sampling the signal  $\bar{y}(t)$  at twice the chip rate, yielding

$$\bar{y}(kT_c) = \sum_n [2x_n(kT_c)\hat{s}^m(kT_c - nT_c) - x_n(kT_c)x^*(kT_c - nT_c) + \hat{\zeta}_n(kT_c)]; \quad (49)$$

$$\bar{y}\left(kT_c + \frac{T_c}{2}\right) = \sum_n \left[ 2x_n\left(kT_c + \frac{T_c}{2}\right)\hat{s}^m\left(kT_c + \frac{T_c}{2} - nT_c\right) - x_n\left(kT_c + \frac{T_c}{2}\right)x^*\left(kT_c + \frac{T_c}{2} - nT_c\right) + \hat{\zeta}_n\left(kT_c + \frac{T_c}{2}\right) \right]; \quad (50)$$

Define

$$\mathbf{y}[k] = \begin{bmatrix} \bar{y}\left(kT_c + \frac{T_c}{2}\right) \\ \bar{y}(kT_c) \end{bmatrix}^T; \quad (51)$$

$$\mathbf{s}^m[k] = \begin{bmatrix} \hat{s}^m\left(kT_c + \frac{T_c}{2}\right) \\ \hat{s}^m(kT_c) \end{bmatrix}^T; \quad (52)$$

$$\boldsymbol{\zeta}[k] = \begin{bmatrix} \hat{\zeta}_n\left(kT_c + \frac{T_c}{2}\right) \\ \hat{\zeta}_n(kT_c) \end{bmatrix}^T, \quad (53)$$

where  $(\cdot)^T$  denotes transposition of matrix. It will be convenient to define the received signal vector  $\mathbf{y}_n$  of length  $2N_g$ , where  $N_g$  is the length of the forward filter for each oversampling polyphase

$$\mathbf{y}_n = \{\mathbf{y}[n]^T \quad \mathbf{y}[n-1]^T \quad \dots \quad \mathbf{y}[n-N_g+1]^T\}^T. \quad (54)$$

Then, the channel input-output relationship can be

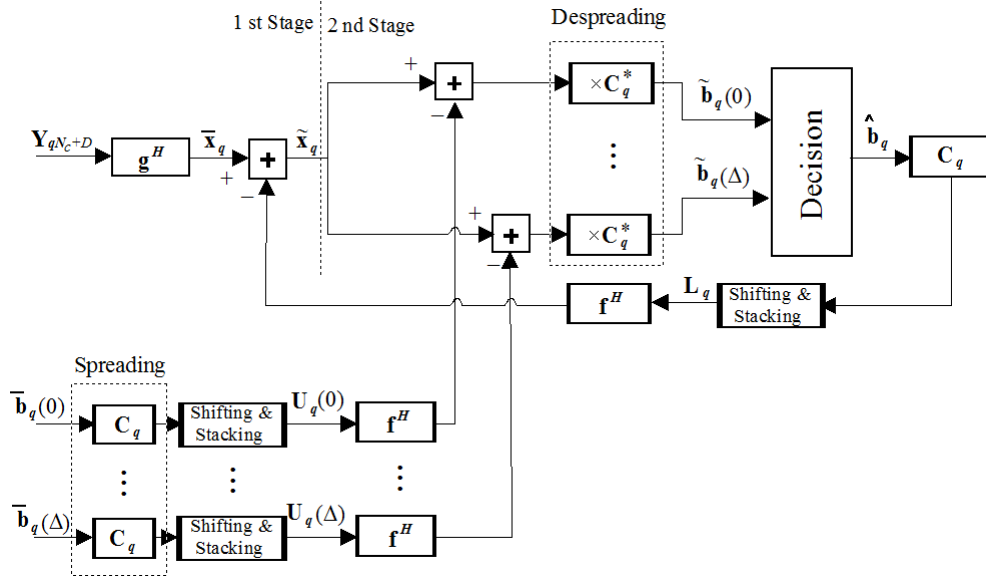


Fig.8. Tentative chip decision feedback equalizer:  $\Delta = 2^{N_d} - 1$ .

expressed as

$$\mathbf{y}_n = 2\mathbf{S}^m \mathbf{x}_n - \mathbf{x}_n \mathbf{x}_n^* + \boldsymbol{\zeta}_n, \quad (55)$$

where  $\mathbf{S}^m$  is the  $2N_g \times (N_g + L - 1)$  convolution matrix and  $\mathbf{x}_n$  is the vectorized synchronous multiuser chip signal

$$\mathbf{S}^m = \begin{bmatrix} \mathbf{s}^m[0] & \cdots & \mathbf{s}^m[L-1] & 0 & \cdots & 0 \\ 0 & \mathbf{s}^m[0] & \cdots & \mathbf{s}^m[L-1] & \cdots & 0 \\ \vdots & \ddots & \ddots & \ddots & \ddots & \vdots \\ 0 & \cdots & 0 & \mathbf{s}^m[0] & \cdots & \mathbf{s}^m[L-1] \end{bmatrix}; \quad (56)$$

$$\mathbf{x}_n = [x_n \ x_{n-1} \ \cdots \ x_{n+2-L-N_g}]^T; \quad (57)$$

$$\boldsymbol{\zeta}_n = \{\boldsymbol{\zeta}[n]^T \ \boldsymbol{\zeta}[n-1]^T \ \cdots \ \boldsymbol{\zeta}[n-N_g+1]^T\}^T \quad (58)$$

and  $L$  is the channel length with contribution of both channel span and raised-cosine waveform extension.

## 5.2 Tentative Chip Decision Feedback Equalizer

The architecture of the tentative chip decision feedback equalizer is presented in Fig. 8 in the form of matrix computations. Compared with [14], we use multiple hypothesis feedback branches to account for combinations of multiple codes. The received signal vectors are stacked to form the block Toeplitz matrix

$$\mathbf{Y}_{qN_c+D} = [\mathbf{y}_{qN_c+D} \ \mathbf{y}_{qN_c+D+1} \ \cdots \ \mathbf{y}_{(q+1)N_c-1+D}], \quad (59)$$

where  $D$  is the estimated system delay. The output of the forward filter takes the following form

$$\bar{\mathbf{x}}_q = \mathbf{g}^H \mathbf{Y}_{qN_c+D} \quad (60)$$

where

$$\mathbf{g} = [g_0 \ g_1 \ \cdots \ g_{2N_g-1}]^T \quad (61)$$

is the forward filter of length  $2N_g$  and  $(\cdot)^H$  denotes the Hermitian transformation of matrix. The  $1 \times N_c$  vector  $\bar{\mathbf{x}}_q$  is the estimate of the multiuser chip signals in the current  $q^{\text{th}}$  symbol interval, i.e.,  $[x_{qN_c} \ x_{qN_c+1} \ \cdots \ x_{(q+1)N_c-1}]$ , but still contains the interference from the post cursors of previous chips.

The decision-feedback signal can be divided into two parts: post cursor chips of previous symbols and the chips of current symbols, respectively. For the first part, the  $N_f \times N_c$  Toeplitz matrix  $\mathbf{L}_q$  consisting of chips of previously decided symbols is formed

$$\mathbf{L}_q = \sum_{j=0}^{N_d-1} \begin{bmatrix} \hat{x}_{qN_c-1}^{(j)} & 0 & \cdots \\ \hat{x}_{qN_c-2}^{(j)} & \hat{x}_{qN_c-1}^{(j)} & \ddots \\ \vdots & \vdots & \ddots \\ \hat{x}_{qN_c-N_f}^{(j)} & \hat{x}_{qN_c-N_f+1}^{(j)} & \cdots \end{bmatrix}. \quad (62)$$

Then the post cursors of previous symbols are filtered by the feedback filter, and cancelled from the received signal by the subtractor shown in the first stage in Fig. 8

$$\tilde{\mathbf{x}}_q = \bar{\mathbf{x}}_q - \mathbf{f}^H \mathbf{L}_q, \quad (63)$$

where

$$\mathbf{f} = [f_0 \ f_1, \dots, f_{N_f-1}]^T \quad (64)$$

is the feedback filter of the length  $N_f$ .

The difficulty of cancelling post cursors of current symbols lies in the fact that the current symbols are still unknown at the time of feeding back; however, it can be overcome by the fact that the symbol alphabet is finite. For example, with the binary phase-shift keying modulation, the symbols are the binary-valued  $b_q^j = \pm 1$ . For  $N_d$  current symbols, the number of all possible combinations is  $2^{N_d}$ . We can construct post cursors corresponding to all these combinations of current symbols, feed them back in parallel branches, subtract them from received signals separately, and despread the outputs of these subtractors. Then, a decision device can be designed to choose the most probable assumption of the current symbols. The above discussion can be mathematically elaborated as the following.

Define a vector containing the current symbols of the desired user

$$\mathbf{b}_q = [b_q^{(0)} \ b_q^{(1)} \ \dots \ b_q^{(N_d-1)}]^T. \quad (65)$$

Denote all possible values of the vector  $\mathbf{b}_q$  as

$$\bar{\mathbf{b}}_q(k) = [\bar{b}_q^{(0)}(k) \ \bar{b}_q^{(1)}(k) \ \dots \ \bar{b}_q^{(N_d-1)}(k)]^T \quad (66)$$

where  $k = 0, 1, \dots, 2^{N_d} - 1$ . Let  $\mathbf{c}_k^j$  be the spreading and scrambling sequence for the  $q$ -th symbol of the  $j$ -th active code

$$\mathbf{c}_k^{(j)} = [c_0^{(j)} s_{qN_c} \ c_1^{(j)} s_{qN_c+1} \ \dots \ c_{N_c-1}^{(j)} s_{(q+1)N_c-1}]^T. \quad (67)$$

Stacking the  $N_d$  code sequences into one matrix, we get

$$\mathbf{C}_q = [\mathbf{c}_Q^{(0)} \ \mathbf{c}_Q^{(1)} \ \dots \ \mathbf{c}_Q^{(N_d-1)}]. \quad (68)$$

For each assumed  $\bar{\mathbf{b}}_q(k), k = 0, 1, \dots, 2^{N_d} - 1$ , we construct the Toeplitz matrix

$$\mathbf{U}_q(k) = \sum_{j=0}^{N_d-1} \bar{b}_q^{(j)}(k) \begin{bmatrix} 0 & c_0^{(j)} s_{qN_c} & \dots & c_{N_c-2}^{(j)} s_{(q+1)N_c-2} \\ 0 & 0 & \ddots & \vdots \\ \vdots & \vdots & \ddots & c_0^{(j)} s_{qN_c} \\ 0 & 0 & \dots & \vdots \end{bmatrix}, \quad (69)$$

whose  $m$ -th column,  $m = 0, 1, \dots, N_c - 1$ , is compressed of  $m$  chips of multicode signals immediately preceding the  $m$ -th chips of the current symbols.

The post cursors are cancelled by filtering  $\mathbf{U}_q(k)$  with the feedback filter  $\mathbf{f}$  and subtracting the result from  $\tilde{\mathbf{x}}_q$ . After despreading, an estimate of the vector  $\mathbf{b}_q$  based on the assumption  $\bar{\mathbf{b}}_q(k)$  is given by

$$\begin{aligned} \tilde{\mathbf{b}}_q(k) &= (1/N_c) [(\tilde{\mathbf{x}}_q - \mathbf{f}^H \mathbf{U}_q(k)) \mathbf{C}_q^*]^T \\ &= (1/N_c) [(\mathbf{g}^H \mathbf{Y}_{qN_c+D} - \mathbf{f}^H \mathbf{L}_q - \mathbf{f}^H \mathbf{U}_q(k)) \mathbf{C}_q^*]^T. \end{aligned} \quad (70)$$

Given  $\tilde{\mathbf{b}}_q(k), k = 0, 1, \dots, 2^{N_d-1}$ , the decision device has to decide on  $\hat{\mathbf{b}}_q(k)$ , the estimate of  $\mathbf{b}_q$ . Of the outputs of  $2^{N_d}$  second-stage subtractors, only one of them corresponds to a correct assumption, and is free of the intersymbol and interchip interferences generated by the post cursors chips of the reference user, while the assumptions of the other subtractors are erroneous in at least one symbol. Since an erroneous assumption in  $b_q^{(j)}$  simply doubles the interchip interferences generated by the  $j$ -th code in the outputs of some subtractors, the Euclidean distance between the assumption-estimate pair  $\bar{\mathbf{b}}_q(k)$  and  $\tilde{\mathbf{b}}_q(k)$  is in general minimized if the assumption is the correct one. Therefore, a minimum-distance rule is used by the decision device

$$\hat{\mathbf{b}}_q(k) = \bar{\mathbf{b}}_q(k_0), \quad (71)$$

where

$$k_0 = \underset{k}{\operatorname{argmin}} \|\bar{\mathbf{b}}_q(k) - \tilde{\mathbf{b}}_q(k)\|, \quad k = 0, 1, \dots, 2^{N_d-1}, \quad (72)$$

where  $\|\cdot\|$  denotes the Frobenius norm.

From the above discussion, among all the branches feeding back the post cursor chips of the current symbols, one and only one of them corresponds to the actual current symbols. The equalizer coefficients are designed to minimize the mean square error between the outputs of this branch's despreading devices and the actual symbols. This explains the assumption that the decisions on past chips are all correct in Section 4.1.

We now derive the discrete-time finite impulse response forward filter coefficients  $g_n$  and the feedback filter coefficients  $f_n$  by assuming that  $\hat{\mathbf{b}}_q$  corresponds to the correct decision, i.e.,  $\hat{\mathbf{b}}_q = \bar{\mathbf{b}}_q(k_0) = \mathbf{b}_q$ . Denote the output of the  $k_0$ -th second-stage subtractor by  $\hat{\mathbf{x}}_q$ , then

$$\hat{\mathbf{x}}_q = \tilde{\mathbf{x}}_q - \mathbf{f}^H \mathbf{U}_q(k_0). \quad (73)$$

The design criterion is to minimize the symbol-level mean square error (*MSE*) given by

$$MSE = E \left| b_q^{(0)} - (1/N_c) \hat{\mathbf{x}}_q \mathbf{c}_q^{(0)*} \right|^2, \quad (74)$$

where we focus on minimizing the mean square error of the zero-th active code. In fact, the filter coefficients are independent of any specific choice of code matrix. From (74) we get

$$MSE = E \left| b_q^{(0)} - (1/N_c) [\mathbf{g}^H \mathbf{Y}_{qN_c+D} - \mathbf{f}^H \mathbf{L}_q - \mathbf{f}^H \mathbf{U}_q(k_0)] \mathbf{c}_q^{(0)*} \right|^2, \quad (75)$$

or

$$MSE = E \left| b_q^{(0)} - \begin{bmatrix} \mathbf{g} \\ -\mathbf{f} \end{bmatrix}^H \left( \frac{1}{N_c} \begin{bmatrix} \mathbf{Y}_{qN_c+D} \\ \mathbf{L}_q + \mathbf{U}_q(k_0) \end{bmatrix} \mathbf{c}_q^{(0)*} \right) \right|^2. \quad (76)$$

Define an augmented coefficient vector for the decision feedback equalizer as

$$\boldsymbol{\omega} = \begin{bmatrix} \mathbf{g} \\ -\mathbf{f} \end{bmatrix} \quad (77)$$

and the vector

$$\boldsymbol{\xi} = \frac{1}{N_c} \begin{bmatrix} \mathbf{Y}_{qN_c+D} \\ \mathbf{L}_q + \mathbf{U}_q(k_0) \end{bmatrix} \mathbf{c}_q^{(0)*}. \quad (78)$$

Then, the symbol-level mean square error becomes

$$E \left| b_q^{(0)} - \boldsymbol{\omega}^H \boldsymbol{\xi} \right|^2 = (\boldsymbol{\omega} - \boldsymbol{\Phi}^{-1} \boldsymbol{\alpha})^H \boldsymbol{\Phi} (\boldsymbol{\omega} - \boldsymbol{\Phi}^{-1} \boldsymbol{\alpha}) + 1 - \boldsymbol{\alpha}^H \boldsymbol{\Phi}^{-1} \boldsymbol{\alpha}, \quad (79)$$

where

$$\boldsymbol{\alpha} = E \{ b_q^{(0)*} \boldsymbol{\xi} \} \quad (80)$$

and

$$\boldsymbol{\Phi} = E \{ \boldsymbol{\xi} \boldsymbol{\xi}^H \}. \quad (81)$$

Thus, the optimal decision feedback equalizer coefficients that minimize the mean square error are

$$\boldsymbol{\omega} = \boldsymbol{\Phi}^{-1} \boldsymbol{\alpha} \quad (82)$$

and the minimum mean square error

$$MSE = 1 - \boldsymbol{\alpha}^H \boldsymbol{\Phi}^{-1} \boldsymbol{\alpha}. \quad (83)$$

From (77) and (82) we get the decision feedback equalizer coefficients as follows:

$$\mathbf{g} = N_c [N_u \mathbf{H} \mathbf{H}^H + (N_c - N_u) \mathbf{h}_{D+1} \mathbf{h}_{D+1}^H + \mathbf{R}_{ww}]$$

$$- N_d \mathbf{H} \mathbf{J}'_D \mathbf{J}_D^H \mathbf{H}^H]^{-1} \mathbf{H} \mathbf{e}_D, \quad (84)$$

$$\mathbf{f} = \mathbf{J}_D^H \mathbf{H}^H \mathbf{g}, \quad (85)$$

where

$$\mathbf{J}_D = \begin{bmatrix} \mathbf{0}_{(D+1) \times N_f} \\ \mathbf{w}_k \\ \mathbf{0} \end{bmatrix} \quad (86)$$

is the  $(N_g + L - 1) \times N_f$  matrix;  $\mathbf{e}_D$  is the vector with one on the  $(D + 1)$ -th position and zeros on all the other positions;  $\mathbf{h}_{D+1}$  is the  $(D + 1)$ -th column of  $\mathbf{H}$ ;

$$\mathbf{R}_{nn} = E \{ \mathbf{w}_k \mathbf{w}_k^H \} \quad (87)$$

is the autocorrelation matrix of the noise vector  $\mathbf{w}_k$ ;  $\mathbf{I}_m$  denotes the  $m \times m$  identity matrix;  $\mathbf{0}_{m \times n}$  represents the  $m \times n$  all-zero matrix. Let  $\mathcal{A}$  be the alphabet of source symbols and  $|\mathcal{A}|$  be its size. The complexity of tentative chip decision feedback equalizer is roughly proportional to  $|\mathcal{A}|^{N_d}$ . Thus, the tentative chip decision feedback equalizer is more appropriate for small alphabet and small  $N_d$ .

### 5.3 Past Symbol Decision Feedback Equalizer

Here we also list the expression of filter coefficients of the past symbol decision feedback equalizer. When only the past symbol decisions are fed back, the symbol-level mean square error has a similar form to that in (76)

$$MSE = E \left| b_q^{(0)} - \begin{bmatrix} \mathbf{g} \\ -\mathbf{f} \end{bmatrix}^H \left( \frac{1}{N_c} \begin{bmatrix} \mathbf{Y}_{qN_c+D} \\ \mathbf{L}_q \end{bmatrix} \mathbf{c}_q^{(0)*} \right) \right|^2. \quad (89)$$

Here,  $\mathbf{L}_q$  appears in place of  $\mathbf{L}_q + \mathbf{U}_q(k_0)$  in (76), i.e. only the contribution of already decided symbols remains. It follows that

$$\mathbf{g} = N_c^2 [N_c N_u \mathbf{H} \mathbf{H}^H + (N_c^2 - N_c N_u) \mathbf{h}_{D+1} \mathbf{h}_{D+1}^H + N_c \mathbf{R}_{ww} - N_d \mathbf{H} \mathbf{J}'_D \mathbf{J}_D^H \mathbf{H}^H]^{-1} \mathbf{H} \mathbf{e}_D; \quad (90)$$

the matrix  $\mathbf{f}$  is given by (85);

$$\mathbf{J}'_D = \begin{bmatrix} \mathbf{0}_{(D+1) \times N_f} \\ \boldsymbol{\Lambda} \\ \mathbf{0} \end{bmatrix}; \quad (91)$$

$$\boldsymbol{\Lambda} = \begin{cases} \text{diag}\{1, 2, \dots, N_f\}, & \text{if } N_f \leq N_c \\ \text{diag}\{1, 2, \dots, N_c, \dots, N_f\}, & \text{otherwise} \end{cases} \quad (92)$$

is the  $N_f \times N_f$  diagonal matrix.

### 5.4 Simulation Results

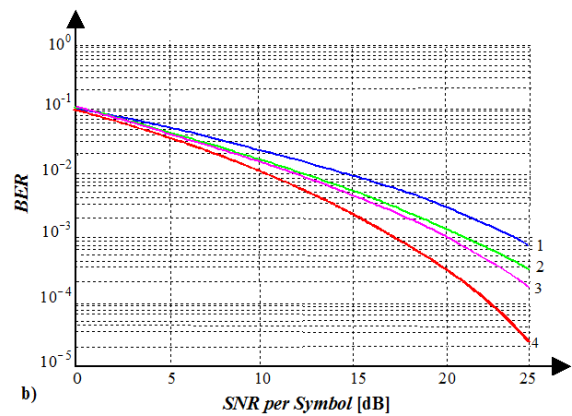
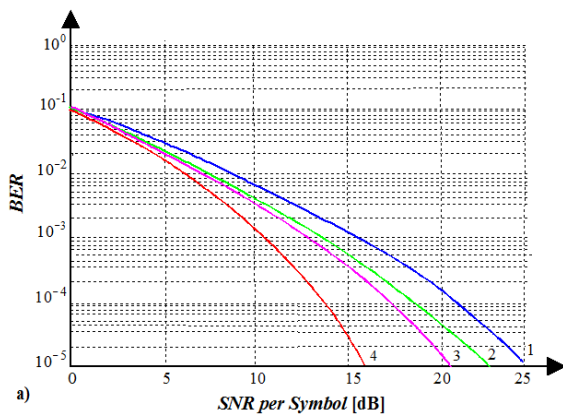
The BER performance of the tentative chip decision feedback equalizer is simulated and compared with the linear equalizer and past symbol decision feedback equalizer. In the simulated wideband CDMA forward link of wireless communication system [18], the chip rate is 3.84 MHz or  $T_c = 0.26 \mu s$ , and the roll-off factor of raised-cosine waveform is equal to 0.22. The scrambling long code is the quaternary phase-shift keying (QPSK) sequence of length 38400 generated according to [3]. The channelization codes are Walsh-Hadamard codes. The spreading factor is  $N_c = 4$ . The data symbols are the binary phase-shift keying, for the sake of simplicity, although QPSK is used in the standard [3]. When computing the coefficients for all equalizers, the system delay  $D$  was chosen to minimize the corresponding mean square error.

For the fixed channel shown in Fig. 4, the BER versus SNR achieved by the linear equalizer, past symbol decision feedback equalizer and tentative chip decision feedback equalizer is shown in Fig. 9 when  $N_d = 1$  and  $N_u$  varies between 1 and 4. For both decision feedback equalizers the length of forward filters is 57 for each oversampling polyphase, same as the length of the linear equalizer. The length of the forward filters and the linear equalizer is chosen in such a way that no further performance improvem-

ent can be observed by increasing the length. The length of the feedback filters is 4, equal to the number of chips of the channel spans. Two decision rules of the tentative chip decision feedback equalizer are presented. The tentative chip decision feedback equalizer 1 corresponds to the decision rule given by (72), while the tentative chip decision feedback equalizer 2 stems from the following minimum-distance rule:

$$\begin{cases} \hat{\mathbf{b}}_q = \bar{\mathbf{b}}_q(k_0), \\ k_0 = \arg \min_k \|\tilde{\mathbf{x}}_q - \mathbf{f}^H \mathbf{U}_q(k) - \mathbf{C}_q \bar{\mathbf{b}}_q(k)\|^2, \\ k = 0, 1, \dots, 2^{N_d} - 1. \end{cases} \quad (93)$$

i.e., the decision symbol vector minimizes the distance between the estimated chips and the desired user's chips of the current symbol. Although it seems that the decision feedback equalizer coefficients should be designed to minimize the chip-level mean square error for this decision rule, our numerical results reveal that the BER curves of the decision feedback equalizer minimizing the chip-level and symbol-level mean square error, respectively, crisscrosses each other in the interested SNR range. Therefore, we apply the decision rule in (93) without deriving a new set of decision feedback equalizer coefficients. It is notable that for the past symbol decision feedback equalizer and linear equalizer the decision rules in (72) and (93) are equivalent.



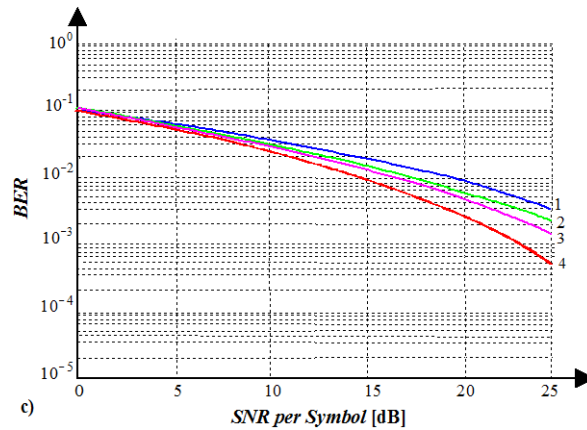


Fig. 9. *BER* of different equalizers over a fixed channel,  $N_d = 1$  while  $N_u$  varies: a)  $N_u = 1$ ; b)  $N_u = 2$ ; c)  $N_u = 4$ ; 1 – linear equalizer; 2 – past symbol decision feed-back equalizer; 3 – tentative chip decision feedback equalizer – decision rule (72); 4 – tentative chip decision feedback equalizer – decision rule (93);

From the figure, both the past symbol decision feedback equalizer and the tentative chip decision feedback equalizer outperform the linear equalizer, but the advantage diminishes as the number of active codes increases. This is because the decision feedback equalizers only suppress the intersymbol interferences and the interchip interferences contributed by the other users when the number of active users is large. It is also shown that the tentative chip decision feedback equalizer performs better than the past symbol decision feedback equalizer, although the difference between the two decision feedback equalizers gets smaller as the number of active users increases. Apparently, the decision rule given by (93) is better than one given by (72) for the tentative chip decision feedback equalizer. In the remaining numerical examples, the tentative chip decision feedback equalizer assumes the decision rule given by (93).

Figure 10 demonstrates the *BER* curves when  $N_d = N_u = 4$ . All other settings are the same as in Fig. 9. The *BER* curve for the tentative chip decision feedback equalizer with  $N_d = N_u = 1$  is also shown in Fig. 10. It can be seen that the tentative chip decision feedback equalizer has a much smaller *BER* than the linear equalizer and past symbol decision feedback equalizer for the simulated *SNR* range. There is no much difference between the performance of the past symbol decision feedback equalizer and the linear equalizer for the medium *SNR* range, which demonstrates that the intersymbol interference in the current symbols is really limiting the accuracy in the decision.

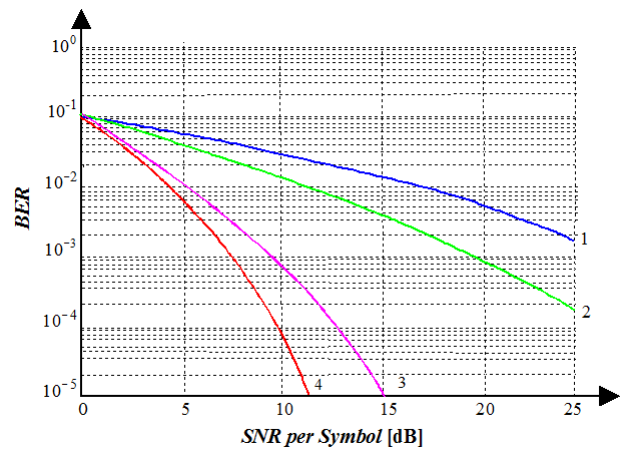


Fig.10. *BER* of different equalizers over a fixed channel.  $N_u = N_d = 4$ ; 1 – linear equalizer; 2 – past symbol decision feed-back equalizer; 3 – tentative chip decision feed-back equalizer; 4 – tentative chip decision feed-back equalizer ( $N_d = N_u = 1$ ).

Figure 11 presents the *BER* simulated on universal mobile telecommunication system indoor office type B channels. The *BER* is averaged over 1000 randomly generated channels. The length of the linear equalizer and the forward filters of decision feedback equalizers are 57. The length of the feedback filters of both decision feedback equalizers is set to be 16, which is slightly larger than the channel span (three chips) plus the extension of the raised cosine waveform (six chips at each side). Also, the *BER* curves of the tentative chip decision feedback equalizer in the case of  $N_u = 1$  are presented. Similarly to Fig. 9 the tentative chip decision feedback equalizer has the best performance among all three equalizers. At the high *SNR* the tentative chip decision feedback equalizer reaches the single-user or code performan-

ce, which agrees with our asymptotic minimum mean square analysis in the last section.

The channels considered above have a span that is comparable to the symbol period. When the channel span is much larger than the symbol period, precursor and post cursor intersymbol interferences account for most part of degradation, while the effect of interchip interferences is relatively insignificant. Thus, the performance advantage of the tentative chip decision feedback equalizer over the past symbol decision feedback equalizer is expected to decrease as the channel span increases. On the other hand, when the channel span is much smaller than the symbol period, the linear equalizer might be enough to counter the effect of multipath, and the complexity of the decision feedback equalizer can be spared.

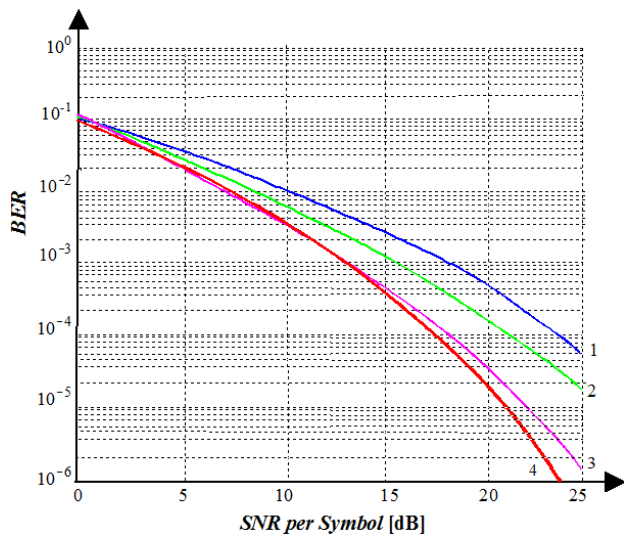


Fig.11. BER of different equalizers over universal mobile telecommunication system indoor office type B channels.  $N_d = N_u = 4$ ; 1 – linear equalizer; 2 – past symbol decision feedback equalizer; 3 – tentative chip decision feedback equalizer; 4 – tentative chip decision feedback equalizer ( $N_d = N_u = 1$ ).

## 6 Conclusions

In the present paper, we analyzed the performance of the ideal decision feedback equalizer that can eliminate the interchip interference caused by the desired user's chip signals. We then apply the tentative chip decision feedback equalizer in the multicode situation to tentatively feed back all possible combinations of the current symbols of the desired user. In all cases, the tentative chip decision feedback equalizer performs better than the linear equalizer and the past symbol decision feedback equalizer. When the desired user owns all active codes, the tentative chip decision feedback equalizer asymptotically

eliminates the multicode interference and approaches the single-user or code performance, similarly to the ideal decision feedback equalizer. The performance is demonstrated through the BER simulation over various channels.

## Appendix I: Proof of (23)

Since the mean square error of decision feedback equalizer  $MSE_{DFE}$  is a functional of  $g(t)$ , we denote it as  $MSE_{DFE}(g)$  here. We now write (23) in detail

$$\begin{aligned}
 MSE_{DFE}(g) = & \int g(\tau)h(-\tau)d\tau \int g^*(s)h^*(-s)ds \\
 & - \int g(\tau)h(-\tau)d\tau - \int g^*(\tau)h^*(-\tau)d\tau + 1 \\
 & + \frac{1}{N_c} \left[ \mathcal{N}_0 \int g(\tau)g^*(\tau)d\tau + (N_u - N_d) \right. \\
 & \times \sum_{n=1}^{\infty} \int g(\tau)h(nT_c - \tau)d\tau \int g^*(s)h^*(nT_c - s)ds \\
 & \left. N_u \sum_{n=-\infty}^{-1} \int g(\tau)h(nT_c - \tau)d\tau \int g^*(s)h^*(nT_c - s)ds \right]. \quad (94)
 \end{aligned}$$

The Gateaux variation [21] of  $MSE_{DFE}(g)$  with regard to  $g$  is

$$\begin{aligned}
 \delta[MSE_{DFE}(g, \nu)] = & \left[ \frac{d[MSE_{DFE}(g + \varepsilon \nu)]}{d\varepsilon} \right]_{\varepsilon=0} \\
 = & 2 \operatorname{Re} \left\{ \int \nu(\tau) \tilde{g}(\tau) d\tau \right\}, \quad (95)
 \end{aligned}$$

where  $\nu(t)$  is the arbitrary function;  $\operatorname{Re}(\cdot)$  means the real part of the quantity in parentheses;

$$\begin{aligned}
 \tilde{g}(t) = & h(-t) \int g^*(\tau)h^*(-\tau)d\tau - h(-t) \\
 & + \frac{1}{N_c} \left[ \mathcal{N}_0 g^*(t) + (N_u - N_d) \sum_{n=1}^{\infty} h(nT_c - T) \right. \\
 & \times \int g^*(\tau)h^*(nT_c - \tau)d\tau + N_u \sum_{n=-\infty}^{-1} h(nT_c - t) \\
 & \left. \times \int g^*(\tau)h^*(nT_c - \tau)d\tau \right] \quad (96)
 \end{aligned}$$

and we have assumed that  $\varepsilon$  is real without loss of generality. A necessary condition for optimal  $g(t)$  to satisfy is that

$$\delta[MSE_{DFE}(g, \nu)] = 0, \quad \forall \nu. \quad (97)$$

Thus, one solution is  $\tilde{g}(t) \equiv 0$ , which implies (23).

## Appendix II: Proof of (31)

Perform the  $z$ -transform of both sides of (24), and we get

$$N_c R(z) = [N_0 + (N_u - N_d)]D(z) + N_d R(z)[D(z)]_+ + (N_c - N_u)d_0 R(z), \quad (98)$$

where

$$[D(z)]_+ = \sum_{n=-\infty}^0 d_n z^{-n}. \quad (99)$$

For the sake of clarity, we denote the optimal solution in (31) as  $\tilde{D}(z)$ , which will be shown to be a solution of (98). Since  $\Gamma(z)$  is the valid power spectrum and can be expressed in the following form

$$\Gamma(z) = \frac{N_d R(z)}{(N_u - N_d)R(z) + N_0} + 1 = \gamma^2 \mathcal{M}(z) \mathcal{M}^*(1/z^*) \quad (100)$$

dividing both sides by  $\gamma^2 \mathcal{M}^*(1/z^*)$  we obtain

$$\begin{aligned} & \frac{N_d R(z)}{(N_u - N_d)R(z) + N_0} \times \frac{1}{\gamma^2 \mathcal{M}^*(1/z^*)} \\ &= \mathcal{M}(z) - \frac{1}{\gamma^2 \mathcal{M}^*(1/z^*)}. \end{aligned} \quad (101)$$

Comparing with (31), we see that  $\tilde{D}(z)$  can be expressed in the following form

$$\begin{aligned} \tilde{D}(z) &= \frac{N_c}{N_d + (N_c - N_u)(1 - \gamma^{-2})} \\ &\times \left[ \mathcal{M}(z) - \frac{1}{\gamma^2 \mathcal{M}^*(1/z^*)} \right]. \end{aligned} \quad (102)$$

Since  $\mathcal{M}(z)$  is causal and  $\mathcal{M}^*(1/z^*)$  is anti-causal, both of them being monic, it follows that

$$[\tilde{D}(z)]_+ = \frac{N_c}{N_d + (N_c - N_u)(1 - \gamma^{-2})} \left[ 1 - \frac{1}{\gamma^2 \mathcal{M}^*(1/z^*)} \right] \quad (103)$$

and

$$\tilde{d}_0 = \frac{N_c(1 - \gamma^{-2})}{N_d + (N_c - N_u)(1 - \gamma^{-2})}. \quad (104)$$

Substituting (31), (103), (104) into the right-hand side of (98), it is easy to show that the equation holds.

## Appendix III: Proof of the Nonincreasing Property of $MMSE_{DFE}(N_d)$

Inspecting (34), we see that the only thing that depends on  $N_d$  is the term  $N_d/[1 - 1/\gamma^2(N_d)]$ , where we have used the notation  $\gamma(N_d)$  to emphasize the dependence of  $\gamma$  on  $N_d$ . To show that  $MMSE_{DFE}(N_d)$  is nonincreasing as  $N_d$  increases, we only need to show that  $N_d/[1 - 1/\gamma^2(N_d)]$  is nonincreasing with  $N_d$ . To achieve this, we form the following difference:

$$\begin{aligned} & \frac{N_d}{1 - 1/\gamma^2(N_d)} - \frac{N_d - 1}{1 - 1/\gamma^2(N_d - 1)} \\ &= \frac{1 + \overline{\Psi(z)}_{\mathcal{G}} - \overline{\Psi(z)} + 1_{\mathcal{G}}}{[1 - 1/\gamma^2(N_d)][1 - 1/\gamma^2(N_d - 1)]}, \end{aligned} \quad (106)$$

Since  $\Psi(z)$  is the valid power spectrum density, it follows from [22] that

$$\overline{\Psi(z)} + 1_{\mathcal{G}} \geq \overline{\Psi(z)}_{\mathcal{G}} + 1. \quad (107)$$

Thus, the nonincreasing property of  $MMSE_{DFE}(N_d)$  is proven.

## References

- [1] T.D.V.A. Naidu, K. Vamsi, Multicode and multicarrier CDMA systems for next generation wireless systems//*International Journal of Scientific & Engineering Research*. 2014, Vol. 5, Issue 9, pp. 931-934.
- [2] N. Guo, L.B. Milstein, on rate-variable multidimensional DS/SSMA with sequence sharing//*IEEE Journal on Selected Areas of Communications*. 1999, Vol. 17, No. 5, pp. 902-917.
- [3] C. Cox, *Essentials of UMTS*. Cambridge University Press: Cambridge, U.K. 2008, 240 pages.
- [4] L. Mailaender, Linear MIMO equalization for CDMA downlink signals with code reuse//*IEEE Transactions on Wireless Communications*. 2005, Vol. 4, No. 5, pp. 2423-2434.
- [5] L. Rugini, Equalization for multicode MC-CDMA downlink channels//*IEEE Communications Letters*. 2012, Vol. 16, Issue 9, pp. 1353-1356.
- [6] K. Mahmood, S. Muhammad Asad, M. Moinuddin, W. Imtiaz, MAI and noise constrained LMS algorithm for MIMO CDMA linear equalizer//*International Journal of Advanced Computer Science and Applications*. 2016, Vol. 7, No. 1, pp. 702-711.
- [7] M. Laxmi Rohini, V. Randa Krishna, Ch. Ga-

- napathy Reddy, Adaptive frequency domain equalization to analyze the effect of carrier frequency offset on SC-CDMA//*International Journal of Engineering Research & Technology*. 2013, Vol. 2, Issue 9, pp. 1400-1405.
- [8] K. Mahmood, Performance comparison between MAI and noise constrained LMS algorithm for MIMO CDMA DFE and linear equalizers// *International Journal of Advanced Computer Science and Applications*. 2016, Vol. 7, No. 12, pp. 405-410.
- [9] G.E. Bottomley, T. Ottosson, Y.-P.E. Wang, A generalized RAKE receiver for interference suppression//*IEEE Journal on Selected Areas of Communications*. 2000, Vol. 18, No. 8, pp. 1536-1545.
- [10] X.Wang, H. Vincent Poor, Blind equalization and multiuser detection in dispersive CDMA channels//*IEEE Transactions on Communications*. 1998, Vol. 46, No. 1, pp. 91-103.
- [11] E. Atify, C. Daoni, A. Boumezzough, A blind identification and equalization for MC-CDMA transmission channel using a new adaptive filter algorithm//*Indonesian Journal of Electrical Engineering and Computer Science*. 2017, Vol. 5, No. 2, pp. 352-362.
- [12] A. Klein, G.K. Kaleh, P.W. Baier, Zero forcing and minimum mean-square-error equalization for multiuser detection in code-division multiple-access channels//*IEEE Transactions on Vehicle Technologies*. 1996, Vol. 45, No. 2, pp. 276-287.
- [13] M. Abdulrahman, A.U.H. Sheikh, D.D. Falconer, Decision feedback equalization for CDMA in indoor wireless communications//*IEEE Journal on Selected Areas of Communications*. 1994, Vol. 12, No. 4, pp. 698-706.
- [14] J.Yang, Y.Li, Tentative chip decision- feedback equalizer for multicode wideband CDMA// *IEEE Transactions on Wireless Communications*. 2005, Vol. 4, No. 1, pp. 137-148.
- [15] F. Adachi, M. Sawahashi, K. Okawa, Tree-structured generation of orthogonal spreading codes with different lengths for forward link of DS-CDMA mobile radio//*Electronics Letters*. 197, Vol. 33, No. 1, pp. 27-28.
- [16] V. Tuzlukov, A new approach to signal detection theory//*Digital Signal Processing: Review Journal*. 1998, Vol.8, No. 3, pp.166–184.
- [17] V. Tuzlukov, *Signal Detection Theory*. Springer-Verlag, New York, USA, 2001, 746 pp.
- [18] V. Tuzlukov, *Signal Processing Noise*. CRC Press, Boca Raton, London, New York, Washington, D.C., USA, 2002, 692 pp.
- [19] M. Maximov, Joint correlation of fluctuative noise at outputs of frequency filters//*Radio Engineering*. 1956, No. 9, pp. 28–38.
- [20] Y. Chernyak, Joint correlation of noise voltage at outputs of amplifiers with no overlapping responses//*Radio Physics and Electronics*. 1960, No. 4, pp. 551–561.
- [21] M. Shbat, V. Tuzlukov, Definition of adaptive detection threshold under employment of the generalized detector in radar sensor systems// *IET Signal Processing*. 2014, Vol. 8, Issue 6, pp. 622–632.
- [22] V. Tuzlukov, DS-CDMA downlink systems with fading channel employing the generalized//*Digital Signal Processing*. 2011. Vol. 21, No. 6, pp. 725–733.
- [23] *Communication Systems: New Research*, Editor: Vyacheslav Tuzlukov, NOVA Science Publishers, Inc., New York, USA, 2013, 423 pp.
- [24] M. Shbat, V. Tuzlukov, Primary signal detection algorithms for spectrum sensing at low SNR over fading channels in cognitive radio//*Digital Signal Processing* (2019). <https://doi.org/10.1016/j.dsp.2019.07.16>. *Digital Signal Processing* 2019, Vol. 93, No. 5, pp. 187- 207.
- [25] V. Tuzlukov, Signal processing by generalized receiver in wireless communications systems over fading channels,” Chapter 2 in *Advances in Signal Processing*. IFSA Publishing Corp. Barcelona, Spain. 2021. pp. 55-111.
- [26] V. Tuzlukov, V. Interference cancellation for MIMO systems employing the generalized receiver with high spectral efficiency//*WSEAS Transactions on Signal Processing*. 2021, Vol. 17, Article #1, pp. 1-15.
- [27] M. Shbat, V. Tuzlukov, SNR wall effect alleviation by generalized detector employment in cognitive radio networks//*Sensors*, 2015, 15(7), pp.16105-16135; doi:10.3390/s150716105.
- [28] V. Tuzlukov, Signal processing by generalized detector in DS-CDMA wireless communication systems with frequency-selective channels//*Circuits, Systems, and Signal Processing*. Published on-line on February 2, 2011, doi:10.1007/s00034-011-9273-1; 2011, Vol.30, No.6, pp. 1197–1230.
- [29] M. Shbat, V. Tuzlukov, Generalized detector as a spectrum sensor in cognitive radio networks// *Radioengineering*. 2015, Vol. 24, No. 2, pp. 558 -571.
- [30] E.A. Lee, D.G. Messerschmitt, *Digital Communication*. 2<sup>nd</sup> Edition, Kluwer: Norwell, MA, USA. 1995.
- [31] J.G. Proakis, M. Salehi, *Digital Communications*. 5<sup>th</sup> Edition, McGraw-Hill Education; New York, USA. 2007, 1150 pages.

- [32] Q.S. Ahmad, S. Ahmad, M.J. Khan, Analysis of simulation parameter of WCDMA for root raised cosine filter//*International Journal of Advanced Research in Computer and Communication Engineering*. 2015, Vol. 4, Issue 8, pp. 473-477.
- [33] V. Wieser, V. Psenak, WCDMA mobile radio network simulator with hybrid link adaptation // *Advances in Electrical and Electronic Engineering*. 2005, No. 3, pp. 200-205.
- [34] J.L. Troutman, *Variational Calculus and Optimal Control: Optimization with Elementary Convexity*. 2<sup>nd</sup> Edition, New York: Springer-Verlag, 1996.
- [35] G.H. Hardy, J.E. Littlewood, G. Polya, *Inequalities*. 2<sup>nd</sup> Edition, Cambridge, U.K.: Cambridge University Press; 1988.



**Dr. Vyacheslav Tuzlukov**

received the MSc and PhD degrees in radio physics from the Belarusian State University, Minsk, Belarus in 1976 and 1990, respectively, and DSc degree in radio physics from the Kotelnikov Institute of Radioengineering and Electronics of Russian Academy of Sciences in 1995. Starting from 1995 and till 1998 Dr. Tuzlukov was a Visiting Professor at the University of San-Diego, San-Diego, California, USA. In 1998 Dr. Tuzlukov relocated to Adelaide, South Australia, where he served as a Visiting Professor at the University of Adelaide till 2000. From 2000 to 2002 he was a Visiting Professor at the University of Aizu, Aizu-Wakamatsu City, Fukushima, Japan and from 2003 to 2007 served as an Invited Professor at the Ajou University, Suwon, South Korea, within the Department of Electrical and Computer Engineering. Starting from March 2008 to February 2009 he joined as a Full Professor at the Yeungnam University, Gyeonsang, South Korea within the School of Electronic Engineering, Communication Engineering, and Computer Science. Starting from March 1, 2009 Dr. Tuzlukov served as Full Professor and Director of Signal Processing Lab at the Department of Communication and Information Technologies, School of Electronics Engineering, College of IT Engineering, Kyungpook National University, Daegu, South Korea. Currently, Dr. Tuzlukov is the Head of Department of Technical Exploitation of Aviation and Radio Engineering Equipment, Belarusian State Academy of Aviation, Minsk, Belarus. His research emphasis is on signal processing in radar, wireless communications, wireless sensor networks, remote sensing, sonar, satellite communications, mobile communications, and other signal processing systems.

He is the author over 280 journal and conference papers, seventeenth books in signal processing published by Springer-Verlag and CRC Press. Some of them are *Signal Detection Theory* (2001), *Signal Processing Noise* (2002), *Signal and Image Processing in Navigational Systems* (2005), *Signal Processing in Radar Systems* (2012), Editor of the book *Communication Systems: New Research* (2013), Nova Science Publishers, Inc, USA, and has also contributed Chapters "Underwater Acoustical Signal Processing" and "Satellite Communications Systems: Applications" to *Electrical Engineering Handbook: 3<sup>rd</sup> Edition*, 2005, CRC Press; "Generalized Approach to Signal Processing in Wireless Communications: The Main Aspects and Some Examples" to *Wireless Communications and Networks: Recent Advances*, InTech, 2012; "Radar Sensor Detectors for Vehicle Safety Systems" to *Electrical and Hybrid Vehicles: Advanced Systems, Automotive Technologies, and Environmental and Social Implications*, Nova Science Publishers, Inc., USA, 2014; "Wireless Communications: Generalized Approach to Signal Processing" and "Radio Resource Management and Femtocell Employment in LTE Networks", to *Communication Systems: New Research*, Nova Science Publishers, Inc., USA, 2013; "Radar Sensor Detectors for Vehicle Safety Systems" to *Autonomous Vehicles: Intelligent Transport Systems and Automotive Technologies*, Publishing House, University of Pitesti, Romania, 2013; "Radar Sensor Detectors for Vehicle Safety Systems," to *Autonomous Vehicles: Intelligent Transport Systems and Smart Technologies*, Nova Science Publishers, Inc., New York, USA, 2014; "Signal Processing by Generalized Receiver in DS-CDMA Wireless Communication Systems," to *Contemporary Issues in Wireless Communications*. INTECH, CROATIA, 2014; "Detection of Spatially Distributed Signals by Generalized Receiver Using Radar Sensor Array in Wireless Communications," to *Advances in Communications and Media Research*. NOVA Science Publishers, Inc., New York, USA, 2015; "Signal Processing by Generalized Receiver in Wireless Communication Systems over Fading Channels" to *Advances in Signal Processing*. IFSA Publishing Corp. Barcelona, Spain. 2021; "Generalized Receiver: Signal Processing in DS-CDMA Wireless Communication Systems over Fading Channels" to *Book Title: Human Assisted Intelligent Computing: Modelling, Simulations and Its Applications*. IOP Publishing, Bristol, United Kingdom, 2022. He participates as the General Chair, Keynote Speaker, Plenary Lecturer, Chair of Sessions, Tutorial Instructor and organizes Special Sections at the major International Conferences and Symposia on signal processing.

Dr. Tuzlukov was highly recommended by U.S. experts of Defence Research and Engineering (DDR& E) of the United States Department of Defence as a recognized expert in the field of humanitarian demining and minefield sensing technologies and had been awarded by Special Prize of the United States Department of Defence in 1999

Dr. Tuzlukov is distinguished as one of the leading achievers from around the world by Marquis Who's Who and his name and biography have been included in the Who's Who in the World, 2006-2013; Who's Who in World, 25<sup>th</sup> Silver Anniversary Edition, 2008, Marquis Publisher, NJ, USA; Who's Who in Science and Engineering, 2006-2012 and Who's Who in Science and Engineering, 10th Anniversary Edition, 2008-2009, Marquis Publisher, NJ, USA; 2009-2010 Princeton Premier Business Leaders and Professionals Honours Edition, Princeton Premier Publisher, NY, USA; 2009 Strathmore's Who's Who Edition, Strathmore's Who's Who Publisher, NY, USA; 2009 Presidential Who's Who Edition, Presidential Who's Who Publisher, NY, USA; Who's Who among Executives and Professionals, 2010 Edition, Marquis Publisher, NJ, USA; Who's Who in Asia 2012, 2<sup>nd</sup> Edition, Marquis Publisher, NJ, USA; Top 100 Executives of 2013 Magazine, Super Network Publisher, New York, USA, 2013; 2013/2014 Edition of the Global Professional Network, Business Network Publisher, New York, USA, 2013;

2013/2014 Edition of the Who's Who Network Online, Business Network Publisher, New York, USA, 2014; Online Professional Gateway, 2014 Edition, Business Network Publisher, New York, USA, 2014; 2014 Worldwide Who's Who", Marquis Publisher, NJ, USA; 2015 Strathmore Professional Biographies, Strathmore's Who's Who Publisher, NY, USA; Who's Who in World, 2015, Marquis Publisher, NJ, USA; 2015-2016 Membership in Exclusive Top 100 network of professionals in the world, NY, USA, 2015; 2015 Who's Who of Executives and Professionals Honours Edition, Marquis Publisher, NJ, USA; Worldwide Who's Who – Top 100 Business Networking, San Diego, CA, USA, 2015.

Phone: +37517345328

Email: [slava.tuzlukov@mail.ru](mailto:slava.tuzlukov@mail.ru)

#### **Contribution of Individual Authors to the Creation of a Scientific Article (Ghostwriting Policy)**

The author contributed in the present research, at all stages from the formulation of the problem to the final findings and solution.

#### **Sources of Funding for Research Presented in a Scientific Article or Scientific Article Itself**

No funding was received for conducting this study.

#### **Conflict of Interest**

The author has no conflict of interest to declare that is relevant to the content of this article.

#### **Creative Commons Attribution License 4.0 (Attribution 4.0 International, CC BY 4.0)**

This article is published under the terms of the Creative Commons Attribution License 4.0

[https://creativecommons.org/licenses/by/4.0/deed.en\\_US](https://creativecommons.org/licenses/by/4.0/deed.en_US)